2nd International Conference on Bio-based Building Materials &
1st Conference on ECOlogical valorisation of GRAnular and FIbrous materials

June 21th - 23th 2017
Clermont-Ferrand, France

ASSESSMENT OF A PRECAST HEMP CONCRETE HYGROTHERMAL PROPERTIES

B. Seng[1,2]*, C. Magniont[1], S. Spagnol[2], S. Lorente[1]

[1] Université de Toulouse, INSA, UPS, Laboratoire Matériaux et Durabilité des Constructions, 31077, Toulouse, France

[2] Université de Toulouse, UPS, Laboratoire Physique de l'Homme Appliquée à Son Environnement, 31062, Toulouse, France

*Corresponding author; e-mail: billy.seng@insa-toulouse.fr

Abstract
The present work aims at measuring the hygrothermal properties of a precast hemp concrete. When available, different experimental techniques were applied to explore the impact of the chosen protocol on the results. The specific heat capacity is assessed through differential scanning calorimetry (DSC) and effusivity measurements. The impact of moisture content on this parameter is then evaluated. The thermal conductivity is the second thermal studied property. The guarded hot plate method is used for measuring the dry thermal conductivity of precast hemp concrete at different temperatures. These results are completed with hot wire measurements which are also used for assessing the impact of water content on the thermal conductivity. As far as the hygric properties are concerned, we measured the sorption isotherm using both the saturated salt solutions method and the Dynamic Vapour Sorption (DVS). Finally, the water vapour permeability was measured applying the dry cup method, a focus was made on the influence of the interface vapour resistance at the top of the cup.

Keywords:
hygrothermal properties, hemp concrete, bio-based material

1 INTRODUCTION

Nowadays, the building sector is the main energy consumer in the developed countries. In France, for instance, residential and commercial buildings represented 45% of the final energy consumption in 2015 [SOeS 2016]. Meanwhile, the future regulations (RBR 2020) prompt to take into account the global environmental impact of buildings: criteria such as life cycle assessment, environmental footprint, health and comfort for indoor environment will become meaningful [Groupe RBR 2024-2050 2014]. In this context, a resurgence of interest in bio-based materials has appeared. Indeed, they have not only less embodied energy but also rely on renewable resource and allow carbon sequestration. Within the different bio-based materials, hemp concrete stands out from the others thanks to hemp agronomic asset. Actually, hemp has a rather high yield, need few plant protection products, herbicides and fertilizers. Hemp concrete is generally used for building envelopes under three possible forms: casted, sprayed on a formwork or pre-fabricated. The latter seems to have the greatest potential of development because it avoids a long drying period during the construction.

Thermal and hygroscopic properties are the main features for energy saving and control of the indoor environment comfort. Such characteristics have been studied experimentally since the 2000s, see for instance Collet et al. [Collet 2013]; Collet and Pretot [Collet 2014a, Collet 2014b]; Evrard [Evrard 2008]; Maalouf et al. [Maalouf 2014]; Walker and Pavía [Maalouf 2014]. Recent studies highlight the dependency of both thermal and hygroscopic properties on temperature and moisture [Aït Oumeziane 2016; Collet 2014a; Rahim 2016a]. Heat and moisture transfers are crucial for energy saving comfort and durability.

Osanyintola and Simonson [Osanyintola 2006] estimated that hygroscopic materials combined with controlled HVAC system can reduce up to 30% the energy consumption. This assessment was confirmed by the numerical study carried out by Woloszyn et al. [Woloszyn 2009] on the combination of moisture-buffering materials and humidity-sensitive ventilation. Direct energy gains were obtained thanks to latent heat exchanges, reducing the heating or cooling demand. However it was highlighted that the main energy savings were achieved through the reduction of the ventilation rate and control of the temperature for similar comfort conditions perceived as with non-hygroscopic materials. In their studies, a relative humidity sensitive ventilation system can reduce the mean ventilation rate up to 30-40% in cold period and can generate 12-17% of energy savings.

Relative humidity (RH) also directly impacts the indoor air quality and then affects the comfort or even the

health of the occupants: for instance, low RH would cause dryness and irritation while high humidities would allow growth of micro-organisms and cause respiratory diseases. With its potential moisture regulation capacity, a hygroscopic material would limit these hazards. In extreme cases, the presence of liquid water because of precipitation, water leakage or interstitial condensation could worsen the material properties and/or damage the material.
Like other bio-based materials, hemp concrete is a hygroscopic material with good insulation properties which ensures relative humidity regulation. Hemp concrete is then adapted to sustainable building, especially for retrofitting since it does not constitute a vapour barrier which can cause moisture damage.

2 MATERIAL

The studied material is a prefabricated vibro-compacted hemp concrete, resulting from previous works performed in LMDC [Dinh 2015; Magniont 2012]. These works focused on the formulation of an innovative pozzolanic binder which led to a patent application.

The dimensions of the hemp concrete brick are approximatively 20 cm x 20cm x 50 cm (See Fig. 1).

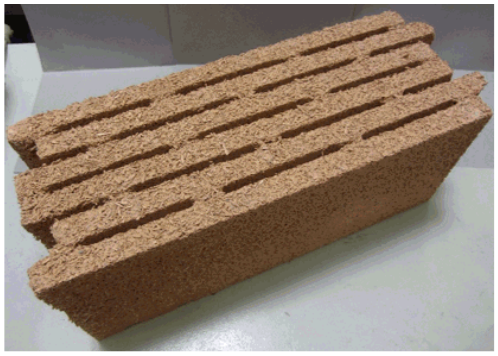

Fig. 7: The hemp concrete precast block.

The binder is composed of lime, metakaolin and superplasticizer additive while the vegetal aggregates are hemp shives.

For the different measurements, samples of different sizes were removed from these blocks (see Tab. 1). Before the measurement or before the stabilization in a fixed relative humidity controlled with a salt solution, they were dried in a laboratory oven at 50°C first. For the vapour permeability tests, the samples were not dried but placed in a climatic chamber (WEISS WK3-2000) at 23°C and 50% relative humidity (RH). The preparation of the samples was considered to be achieved when the sample mass change was less than 0.1% between two weighings within at least 24 hours interval. For the DSC experiments, hemp and binder crushed samples passing through an 80 µm sieve were prepared

The physical properties were measured: the mean apparent density of hemp concrete is $\rho_{a,HC}$=466±25 kg.m^{-3}. Hydrostatic weighing gave the solid density of the main components (hemp and binder) and of the hemp concrete itself (ρ_{hemp}=1452±10 kg.m^{-3}, ρ_{binder}=2305±10 kg.m^{-3} and ρ_{HC}=2149±9 kg.m^{-3}). It was then possible to evaluate the mass ratios x_i(-) of the component i ($x_i=m_i/m_{HC}$) thanks to the mass and volume conservation equations (Eq. (1) and (2)):

$$x_{hemp} = (\rho_{binder} - \rho_{HC})/(\rho_{binder} - \rho_{hemp}) \quad (1)$$

$$x_{binder} = 1 - x_{hemp} \quad (2)$$

Thus, the mass ratios of the components were found: x_{hemp}=0.12±0.04 and x_{binder}=0.88±0.04.

Knowing the different densities, it was also possible to calculate the porosity of the material (Eq. (3)):

$$\varepsilon_{tot} = 1 - \rho_{a,HC}/\rho_{HC} \quad (3)$$

A porosity of ε_{tot}=0.78±0.05 was found.

3 EXPERIMENTAL METHODS AND THEORY

3.1 Sorption isotherm

Saturated salt solution method

The sorption isotherm expresses the amount of moisture in a material when the latter is in equilibrium with its environment.

Based on NF EN ISO 12571 [AFNOR 2013], the sorption isotherms were measured at 23°C. After drying, the samples were put in a ventilated box with a saturated salt solution. All the boxes were placed in a climatic chamber in order to maintain the temperature constant. Five relative humidities were considered (Tab. 2). Eight samples were initially inserted in each box. In time, the hygroscopic samples reached a mass equilibrium due to adsorption/desorption phenomena. Equilibrium was considered to be reached when the change of mass between three consecutive weighings with at least 24h interval, was less than 0.1% of the total mass. The moisture content u (-) was calculated (Eq. (4)):

$$u = (m - m_{dry})/m_{dry} \quad (4)$$

where m is the mass of the sample in equilibrium (g) and m_{dry} is the mass of the dry sample (g).

Tab. 1: Weighing scale and sample geometry information.

Studied parameter	Weight stabilization monitoring: Scale /precision		Shape / dimensions
Thermal conductivity (GHP & Hot wire)	Sartorius CPA 4202 S	10^{-2} g	GHP: Rectangular 15x15x2.5cm^3 Hot wire: Rectangular 25x10x2.5cm^3
Specific heat capacity (Effusivity)			Rectangular 25x10x2.5cm^3
Specific heat capacity (DSC)	Sartorius LP 620 P	10^{-3} g	Powder < 80µm
Sorption isotherm	Precisa XT 620M	10^{-3} g	Rectangular 6x10x2.5cm^3
Vapour permeability			Cylindrical: diameter=11 cm, height=2.5cm

Tab. 2: Relative humidities and their saturated salt solutions used in the study [AFNOR 2013].

Relative humidity (NF EN ISO 12571)	Saturated salt solution
7.98±1.9 %	Sodium hydroxide NaOH
32,9±0.17 %	Magnesium chloride $MgCl_2$
75.36±0.13 %	Sodium chloride NaCl
94.00±0.60 %	Potassium nitrate KNO_3
97.42±0.47 %	Potassium sulfate K_2SO_4

Many models, based on physical or mathematical theories, have been developed for describing this parameter. They are convenient for modeling and simulation of heat and moisture transfers. One of the most common model, the GAB model (Guggenheim, Andersen, de Boer) [Anderson 1946], is convenient for describing the isotherm in a wide range of relative humidity. Its expression is (Eq. (5)):

$$u = \frac{u_m \cdot C \cdot K \cdot \Psi}{(1 - K \cdot \Psi)(1 + K(C-1)\Psi)} \quad (5)$$

where ψ is the relative humidity (-) ; u_m, C and K are fitting coefficients (-).

DVS

Dynamic Vapour Sorption (DVS) is also a gravimetric method initially used in pharmaceutical and agrofood industry.

The sample is set in a crucible, attached to a microbalance. The resulting system is in a closed chamber where temperature and relative humidity can be controlled, by mixing nitrogen gas and water vapour (see Fig. (2)):

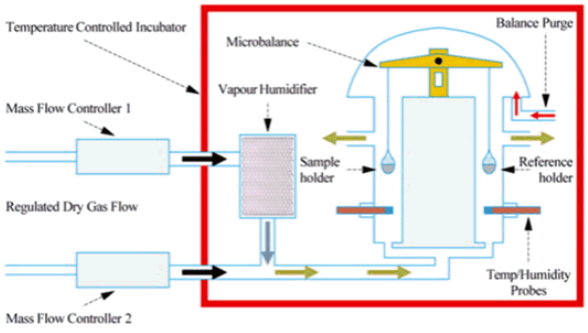

Fig. 8: Scheme of the DVS device, based on [Surface Measurement Systems 2000]

Prior to the measurement, a preheating was performed for two hours around 0% RH. Then a sorption was set, by step of 10% RH with an additional step at 95% RH. The mass of the sample was continuously monitored. The stabilization criteria (dm/dt) was set at 10^{-4} %.min^{-1} and by duration criteria (6 hours for RH<80%, 12h for 80%<RH<90% and 18h for RH=95%).

The masses of the two tested samples were around 330 mg and 160mg.

3.2 Water vapour permeability

The water vapour permeability δv (kg.m^{-1}.s^{-1}.Pa^{-1}) is the capacity of a material to let water vapour go through it, under a difference of vapour pressure.

The measurement of this parameter was based on NF EN ISO 12572 [AFNOR 2016] with the so called cup method with saturated salt solution (SSS) (see Fig. 3).

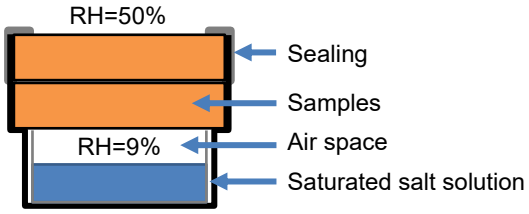

Fig. 9: Scheme of cup method for vapour permeability measurement.

A solution of saturated sodium hydroxide (NaOH) was put in the bottom of the cup, setting an inside relative humidity of around 9%. Then several layers of hemp concrete were inserted: two total thicknesses were tested: around 5 cm (2 layers of material) and around 8 cm (3 layers). The overall system was sealed with a mixture of wax and paraffin. The cups were then put into a climatic chamber at a temperature of 23°C and 50% relative humidity. By controlling the position of the cup inside the climatic chamber, it was possible to adjust the air velocity above the cup: this velocity was measured with a hot-wire anemometer. Consequently, two air velocities were tested: around 2 m.s^{-1} (referred as 'high' velocity) and around 0.5 m.s^{-1} (referred as 'low' velocity).

The cups were regularly weighted until steady state was reached, i.e. when the mass gain G (kg.s^{-1}) (Eq. (6)) was constant.

$$G = \Delta m / \Delta t \quad (6)$$

where Δm is the increase of the mass due to moisture absorption (kg) in the system during Δt (s).

The vapour flux density g_v (kg.m^{-2}.s^{-1}), defined in Eq. (7) is then linked to the apparent vapour permeability $\delta_{v,app}$ (kg.m^{-1}.s^{-1}.Pa^{-1}) (Eq. (8)) or with the expression of the apparent vapour resistance Z_{app} (m^2.s.Pa.kg^{-1}) (Eq. (9)), based on a Fick's law assumption:

$$g_v = G / A \quad (7)$$

$$g_v = \Delta p_v \cdot (\delta_{v,app} / d) \quad (8)$$

$$g_v = \Delta p_v / Z_{app} \quad (9)$$

Where A is the exposed area (m^2), d the total thickness of the material (m), Δp_v is the difference of vapour pressure across the samples (Pa).

Actually, the apparent vapour resistance Z_{app} is composed of the interface vapour resistance Z_{int} at the top of the cup, the air layer vapour resistance Z_{air} and the material vapour resistance R_{mat}, (Eq. (10) and (11)):

$$Z_{app} = Z_{int} + Z_{mat} + Z_{air} \quad (10)$$

$$g_v = \frac{1}{Z_{int} + Z_{mat} + Z_{air}} \Delta p_v \quad (11)$$

We can define the two former resistances as:

$$Z_{int} = 1 / h_m \quad (12)$$

$$Z_{air} = d_{air} / \delta_{air} \quad (13)$$

where h_m is the mass transfer coefficient (s.m^{-1}), d_{air} is the thickness of the air layer (m) and δ_{air} is the vapour permeability in air (kg.m^{-1}.s^{-1}.Pa^{-1}).

When the interface resistance is neglected, as it is stated in NF EN ISO 12572 [AFNOR 2016], the vapour permeability of the material $\delta_{v,mat}$ can be then estimated when taking in account the air layer only (Eq. (14)):

$$\delta_{v,mat} = \frac{d}{\frac{\Delta p_v}{g_v} - \frac{d_{air}}{\delta_{air}}} \quad (14)$$

The permeability of a material can also be characterized by the water vapour resistance μ (-) and the water vapour diffusion-equivalent air layer thickness S_d (m). They are both related to water vapour permeability δ_v and the thickness of the material d (m) (Eq. (15) and (16)):

$$\mu = \delta_{v,air} / \delta_v \quad (15)$$

$$\delta_d = (\delta_{v,air} / \delta_v) \cdot d \quad (16)$$

where $\delta_{v,air}$ is the water vapour permeability in air, equal to 1.98 10^{-10} kg.m^{-1}.s^{-1}.Pa^{-1} at 23°C.

3.3 Thermal conductivity

The thermal conductivity λ (W.m^{-1}.K^{-1}) is the ability of a material to conduct heat under a gradient of temperature.

Steady-state thermal conductivity measurement

The measurement of the thermal conductivity in steady state was performed with a λ-Meter EP500 guarded hot plate (GHP). In this apparatus, a hot plate and a cold plate surround the sample and then create a heat transfer rate through the sample (see Fig. 4). Knowing this heat rate and the geometry of the sample, it is possible to obtain the thermal conductivity using the Fourier's law of conduction.

The measurements were performed on six different dry samples at the mean temperature of 10°C, 23°C and 40°C. The temperature difference between the two plates was set at 5°C.

Transient state thermal conductivity measurement

The transient thermal conductivity was measured with a Neotim FP2C thermal conductivimeter using a hot wire.

The probe, composed of an electric resistance and a thermocouple, is placed between two samples (see Fig. 5). The resistance creates an increase of temperature and the thermocouple measures this increase. Then, solving the heat conduction equation in cylindrical coordinate, assuming a semi-infinite material, the thermal conductivity can be determined.

Some samples were conditioned at a specific relative humidity; namely 50%, 65% and 95% RH; allowing the evaluation of thermal conductivity according to the moisture content.

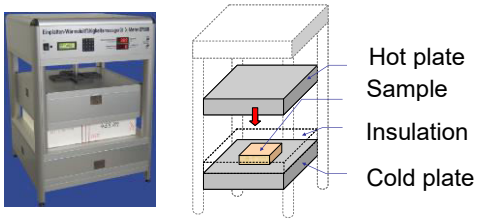

Fig. 10: Guarded hot plate (GHP)- λ-Meter EP500.

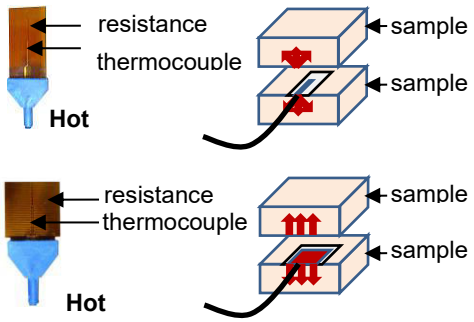

Fig. 11: Hot wire and hot plane schemes.

3.4 Specific heat capacity

The specific heat capacity c_p (J.kg^{-1}.K^{-1}) is the capacity of a material to store thermal energy.

DSC measurement

The measurement of the specific heat capacity was performed with the NEZTSCH STA 449 F3 Differential Scanning Calorimetry (DSC) apparatus, and is based on NF EN ISO 11357-4 [AFNOR 2014]. The apparatus contains two crucibles in its oven: a reference one which is always empty and the one which contains the studied materials. The measurement requires three cycles: a "blank" cycle (both crucibles are empty) that avoids the defects of the system, a "standard" cycle in order to obtain the signal for a reference material, namely a sapphire, and finally a "sample" cycle, in which the studied material is tested.

When the temperature increase of ΔT (K) for the period Δt, the specific heat capacity $c_{p,i}$ (J.kg^{-1}.K^{-1}) of a material i of mass m_i (kg) is linked to the heat rate Q_i (W) according to Eq. (17):

$$Q_i = m_i \cdot c_{p,i} \cdot \Delta T / \Delta t \quad (17)$$

Then, the apparatus does not have access directly to the heat rate Q_i but to a DSC signal proportional to the latter. For the sapphire and the sample cycles, the obtained DSC signal (DSC_i in μV) corrected by the blank one (DSC_b) is then DSC_i-DSC_b (Eq. (18)):

$$DSC_i - DSC_b \propto m_i \cdot c_{p,i} \cdot \Delta T / \Delta t \quad (18)$$

If we consider Eq. (18) for the sapphire (referred by the subscript *st* for "standard") and the sample (referred by the subscript *s*), dividing the latter by the former, we obtain the regular expression of the specific heat capacity of a studied sample $c_{p,s}$ measured with a DSC (Eq. (19)):

$$c_{p,s} = c_{p,st} \cdot (m_{st} / m_s) \cdot (DSC_s - DSC_b) / (DSC_{st} - DSC_b) \quad (19)$$

Four samples of hemp and three samples of binder in powder were tested, as presented in Section 2.

Indirect evaluation through effusivity measurement

The effusivity b (J.m^{-2}.K^{-1}.s$^{-1/2}$) shows the tendency of a body to exchange heat with another by surface contact.

This parameter is measured by the Neotim FP2C equipped with a hot plane probe. Similarly to the thermal conductivity, the effusivity is obtained by solving the unsteady heat conduction equation, assuming semi-infinite material and unidirectional flux.

Knowing the effusivity, the specific capacity can be evaluated according to Eq. (20):

$$b = (k \cdot \rho \cdot c_p)^{1/2} \quad (20)$$

where k is the thermal conductivity (W.m^{-1}.K^{-1}), ρ is the apparent density of the material (kg.m^{-3}).

4 RESULTS AND DISCUSSION

4.1 Sorption isotherm

Fig. (6) shows the results of the sorption isotherm with the fitted GAB model for both saturated salt solution (SSS) method and DVS method. The fitting was obtained with a least squares method on the whole range. Thus, the fitting parameters were u_m=0.01, C=4.52 and K=0.91 for saturated salt solution method and u_m=0.02, C=117.94 and K=0.91 for DVS method.

We can draw attention to the very small scattering among the different samples moisture content in the saturated salt solution method (for each relative humidity, only one sample was removed due to its disjointed mass stabilization); while a large discrepancy appeared in the DVS measurement. This issue highlights the representativeness of this method, even though only two samples were tested. Moreover, the stabilization in the DVS device is troublesome, as the duration criteria was dominant. Therefore, the uncertainties in high RH have to be all the more taken with caution. However, the environment parameters (temperature and RH) should be more precisely controlled in the DVS device by its construction, avoiding for example the exposure of the sample to ambient environment at the time of weighing.

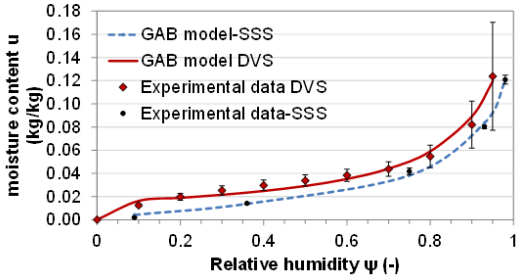

Fig. 12: Sorption isotherm of hemp concrete at 23°C.

4.2 Vapour permeability

Tab. (3) presents the results of the vapour permeability measurements calculated from the resistance of the air layer inside the cup (Eq. (14)). The obtained water vapour resistance factor μ is lower than the literature values: Evrard and De Herde [Evrard 2010] used a value of 4.85, and Rahim et al. [Rahim 2016b] recently found a μ=8.98 for their hemp concrete. Collet et al. [Collet 2013] measured a μ=6.8, while Walker and Pavía [Walker 2014] found for different formulations a vapour resistance factor between 5.4 and 5.7. Nevertheless, in these last references, the authors did not precise if they considered the resistance of the air layer into the cup.

In the present study, the water vapour diffusion-equivalent air layer thickness (S_d) of the samples was slightly higher than the limit of 0.1 m established in the NF EN ISO 12572 [AFNOR 2016]. Nevertheless, for these highly permeable materials, as suggested by Vololonirina and Perrin [Vololonirina 2016], the measurement of vapour permeability can be significantly affected by the interface resistance at the top of the cup. Additional measurements were then conducted. As seen in Tab. (3), in the second series of measurements, the reduction of the air velocity at the top of the cup (from 2 to 0.5 m/s) significantly decreases the apparent permeability of the material, due to the additional resistance of the air layer. The third series of measurements, made with a high air velocity, but on samples with distinct thickness, allowed the estimation of the interface resistance, applying the following method based on the approach presented by Vololonirina and Perrin [Vololonirina 2016].

Knowing the air layer in each cup, it was possible to estimate Z_{int}+Z_{mat} (Eq. (21)):

$$Z_{\text{int}} + Z_{mat} = Z_{app} - Z_{air} \quad (21)$$

When the thickness tends toward zero, the sum Z_{int}+Z_{mat} tends toward Z_{int} as described in Eq. (22). Thus, Z_{int} is estimated around 1.49x10^8 m.s^{-1}.

$$\lim_{d \to 0} \left(Z_{\text{int}} + Z_{mat}\right) = \lim_{d \to 0} \left(\frac{1}{h_m} + \frac{d}{\delta_{mat}} \right) = \frac{1}{h_m} \quad (22)$$

Knowing Z_{int}, the material vapour resistance can be calculated:

$$Z_{mat} = Z_{app} - Z_{air} - Z_{\text{int}} \quad (23)$$

Tab. 3: Vapour permeability experimental results and calculations.

	2 layers of mat.		3 layers of mat.
Thickness (m)	0.05	0.05	0.08
Air velocity (m.s^{-1})	'High'	'Low'	'High'
Standard calculation (NF EN ISO 12572 [AFNOR 2016]) taking into account the resistance of the air layer			
$\delta_{v,mat}$ (kg.m^{-1}.s^{-1}.Pa^{-1})	9.7 10^{-11} ± 6.7 10^{-12}	8.6 10^{-11} ± 1.46 10^{-11}	1.1E-10 ± 1.3 10^{-11}
μ_{mat} (-)	2.06 ± 0.14	2.34 ± 0.35	1.86 ± 0.23
Taking into account all the resistances			
Z_{app} (m^2.s.Pa.kg^{-1})	6.40 10^8 ± 3.51 10^7	6.90 10^8 ± 1.25 10^8	8.43 10^8 ± 1.01 10^8
Z_{air} (m^2.s.Pa.kg^{-1})	8.94 10^7 ± 1.63 10^6	7.57 10^7 ± 2.18 10^7	8.71 10^7 ± 1.05 10^6
Z_{int} (m^2.s.Pa.kg^{-1})	1.49 10^8	-	1.49 10^8
Z_{mat} (m^2.s.Pa.kg^{-1})	4.02 10^8 ± 3.46 10^7	-	6.07 10^8 ± 1.02 10^8
$\delta_{v,mat}$ (kg.m^{-1}.s^{-1}.Pa^{-1})	1.33 10^{-10}	-	1.34 10^{-10}
μ_{mat} (-)	1.50 ± 0.13	-	1.50 ± 0.25

All the results are presented in Tab. (3). According to this last method the vapour permeability appears to be 31% greater than the vapour permeability calculated neglecting the interface resistance of the air layer at the top of the cup. Theses vapour permeabilities seemed quite high. Further experiments with different thickness (adding 4 layers of material for instance) and air velocities would bring better precision to this method.

4.3 Thermal conductivity

Fig. (7) confronts the thermal conductivity measured with hot-wire and GHP with the literature values.

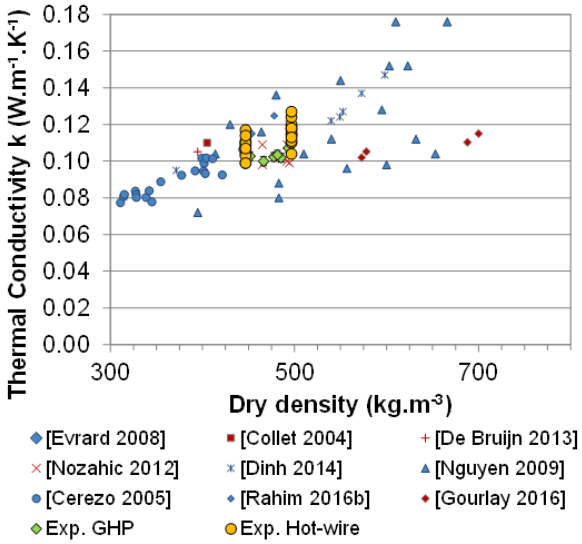

Fig. 13: Dry thermal conductivity as function of density (GHP and hot box: blue, hot wire and hot plane: red).

With GHP measurements, we obtained a mean value of k_{dry}=0.103±0.002 W.m^{-1}.K^{-1} while hot-wire measurement led to k_{dry}=0.112±0.007 W.m^{-1}.K^{-1}. Based, on literature results hereinbefore, no general trend can be drawn concerning the impact of the method on the measurement of this parameter.

Fig. 8 shows the thermal conductivity with dependency on humidity, measured with hot wire device. The self-consistent scheme (SCS) is applied on these experimental results. This model, commonly used on building materials and hemp concrete [Boutin 1996; Collet 2014a; Rahim 2016a] allows the evaluation of the effective thermal conductivity of an heterogeneous material, i.e. with different phases such as air (*a*), water (*w*) and solid phases (*s*). It was based on a concentric spherical inclusion assumption, with R radius for each phase (Fig. (9)).

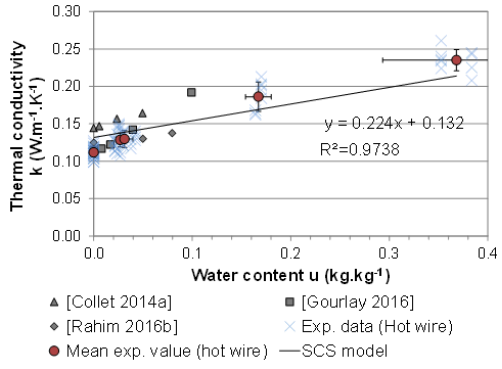

Fig. 8: Thermal conductivity: experimental measurements and SCS model.

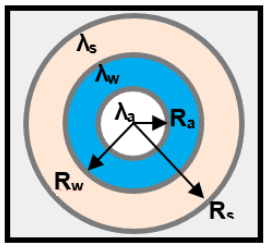

Fig. 9: Three-phase composite sphere in self-consistent model [Boutin 1996]

The resulting expression of the SCS model is:

$$k_{eq} = k_s \left(1 + \frac{n}{\left(\frac{1-n}{3} + \frac{3 + \delta(k_a/k_w - 1)}{3(k_a/k_s - 1) - \delta(k_a/k_s - 1)(2k_w/k_s - 1)} \right)} \right) \quad (24)$$

with $n = \varepsilon$, ε is the porosity and $\delta = u \cdot \rho_{app,HC} / (\rho_w \cdot \varepsilon)$ where u is the water content (kg/kg), $\rho_{a,HC}$ is the hemp concrete apparent density (kg.m^{-3}), ρ_w is the water density (kg.m^{-3}). The obtained relation according to the SCS model is:

$$k(u) = 0.224 \cdot u + 0.132 \quad (25)$$

There was a good agreement with literature value: [Collet 2014a; Rahim 2016a] found respectively according to SCS model, k(u)=0.208·u+0.149 and k(u)=0.258·u+0.126.

4.4 Specific heat capacity

Fig. (10) shows the specific heat capacity DSC measurements of hemp shives and binder with temperature dependency, compared to some biomass material literature values. There are quite few measurements of the specific heat capacity of hemp concrete and its component found in the literature. The dependency on the temperature is even scarcer. Thus Fig. (10) leans on the measurement of c_p of other biomass material and gives above all an order of magnitude: Dupont et al. [Dupont 2014] and Damfeu et al. [Damfeu 2016] studied several of them using also a DSC device: the material presented were retained as extreme values of their respective study. We can observe that the specific heat capacity of hemp stands in the range of the other biomass materials, and as it is observed in the literature, there was a linear dependency between the thermal capacity and temperature. The increase of the specific heat capacity in temperature was however slightly higher in our measurements: $c_{p,hemp}$=7.84·T+1067 with R^2=0.99 and $c_{p,binder}$=3.10·T+798 with R^2=0.99.

The temperature range was above ambient temperature, as it can be found in the literature, due to a lack of precise control with cooling system in such device for the moment.

The specific heat capacity of the hemp concrete can be deduced from Eq. (26):

$$c_{p,HC}^{dry} = x_{hemp} \cdot c_{p,hemp} + x_{binder} \cdot c_{p,binder} \quad (26)$$

Therefore, if we extrapolate the mean specific heat capacity, with a mean standard deviation to 20°C: $c_{p,hemp}$=1224±62 J.kg^{-1}.K^{-1}, $c_{p,binder}$=859±31 J.kg^{-1}.K^{-1}. And the resulting specific heat capacity of hemp concrete is: $c_{p,HC(DSC)}^{dry} = 915 \pm 118 \ J.kg^{-1}.K^{-1}$ at 20°C.

On the other hand, the measured effusivity was b=197±16 J.m^{-2}.K^{-1}.s$^{-1/2}$. Knowing the thermal conductivity k_{dry}=0.112±0.007 W/(m K) and the apparent density $\rho_{a,HC}$=466±25 kg/m³; the specific heat capacity can be calculated according to Eq. (20): $c_{p,HC(hotplane)}^{dry} = 741 \pm 86 \ J.kg^{-1}.K^{-1}$. Assuming that the room temperature during the effusivity measurement was around 20°C, there was a difference of 23% between both methods.

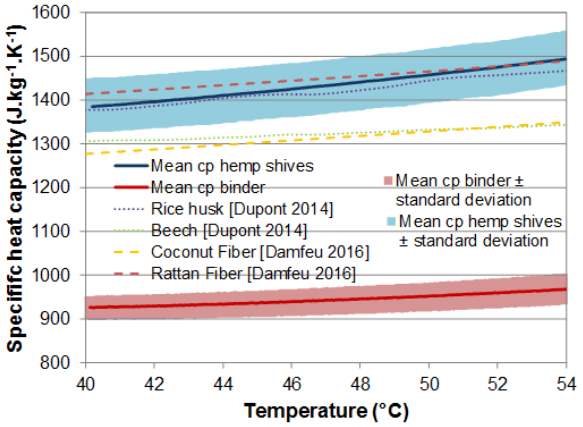

Fig. 10: Specific heat capacity of hemp shives and binder as function of temperature.

Knowing the dry specific heat capacity of hemp concrete, it is then possible to evaluate the wet specific heat capacity (Eq. (27)):

$$c_{p,HC}^{wet} = \left(\frac{1}{1+u}\right) c_{p,HC}^{dry} + \left(\frac{u}{1+u}\right) c_{p,water} \quad (27)$$

The results remain in the range of the literature values where a large scattering is observed (Fig. (11)): with calculations from measurements using a hot plane, Collet [Collet 2004] found 1000 J.kg^{-1}.K^{-1} and Pierre et al. [Pierre 2013] found 650 and 870 J.kg^{-1}.K^{-1}; with a calorimeter, Walker and Pavía [Walker 2014] obtained value from 1240 to 1350 J.kg^{-1}.K^{-1} for hemp concrete with different binders and Evrard [Evrard 2008] found 1560 J.kg^{-1}.K^{-1}. This last author also calculated the wet specific heat capacity of hemp concrete. The specific capacities from the previous measurements are presented as function of water content according to Eq. (27).

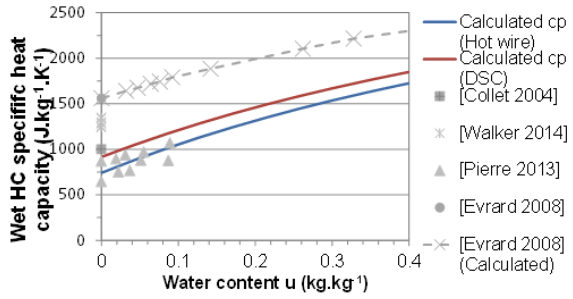

Fig. 11: Calculated value of the specific heat capacity as function of water content.

5 CONCLUSION AND PERSPECTIVES

A complete hygrothermal characterization of a precast hemp concrete was presented in this paper.

For the hygric properties, the sorption isotherm was measured at 23°C with two methods: standard method with saturated salt solution and with DVS method. This last method should allow better control of the temperature and RH but shows few limitations with regards to representativeness and stabilization duration which could require more time than expected. The impact of temperature is currently under investigation, as the literature suggests the dependency of this parameter on sorption for bio-based material [Colinart 2017; Le 2015].

The vapour permeability was measured with the dry cup method. The calculation was performed according to NF EN ISO 12572 [AFNOR 2016] and showed a high value of vapour permeability compared to literature ones. As the material appeared to be very permeable, a different approach of calculation, based on the work of Vololonirina and Perrin [Vololonirina 2016], was proposed; highlighting the impact of the interface resistance at the top of the cup. Indeed, it is possible that this last one can not be neglected for permeable material. Further measurements with additional thickness of material and air velocity should be performed in order to investigate this approach.

In terms of thermal properties, the thermal conductivity was measured with both hot-wire and GHP method. The impact of humidity was estimated experimentally and with the application of the self-consistent scheme.

The specific heat capacity was tackled with two approaches: indirect measurement through the effusivity measurement and with DSC method on the components. The results are consistent with literature value, a little bit less with the indirect method which lead to a lower specific heat capacity. Further measurement on monolithic sample could confirm the approach with the DSC method, allowing the estimation of a composite material when the composition is known. By calculation, the impact of water content can also be obtained.

These experimental results and the importance of temperature and humidity interdependency will be verified experimentally in wall scale with a bi-climatic chamber. These parameters will be included in a sensitivity analysis in modelling the hygrothermal transfer at wall scale.

6 ACKNOWLEDGMENTS

The authors would like to acknowledge the SEAC company which provided the materials for this study and the scientific project neOCampus, lead by Paul Sabatier University Toulouse III which supports these works.

7 REFERENCES

[AFNOR 2013] AFNOR; Hygrothermal performance of building materials and products — Determination of hygroscopic sorption properties; NF EN ISO 12571, 2013.

[AFNOR 2014] AFNOR; Plastics — Differential scanning calorimetry (DSC) — Part 4: Determination of specific heat capacity; NF EN 11357-4, 2014.

[AFNOR 2016] AFNOR; Hygrothermal performance of building materials and products — Determination of water vapour transmission properties — Cup method; NF EN12572, 2016.

[Aït Oumeziane 2016] Aït Oumeziane, Y., Moissette, S., Bart, M., Lanos, C.; Influence of temperature on

sorption process in hemp concrete. Construction and Building Materials, 2016, 106, 600–607.

[Anderson 1946] Anderson, R.B.; Modifications of the Brunauer, Emmett and Teller Equation. Journal of the American Chemical Society, 1946, 68, 686–691.

[Boutin, 1996] Boutin, C.; Conductivité thermique du béton cellulaire autoclavé: modélisation par méthode autocohérente. Mat. Struct. 1996, 29, 609–615.

[Cerezo 2005] Cerezo, V.; Propriétés mécaniques, thermiques et acoustiques d'un matériau à base de particules végétales: approche expérimentale et modélisation théorique. ENTPE, 2005.

[Colinart 2017] Colinart, T., Glouannec, P; Temperature dependence of sorption isotherm of hygroscopic building materials. Part 1: Experimental evidence and modeling. Energy and Buildings, 2017 139, 360–370.

[Collet 2004] Collet, F; Caractérisation hydrique et thermique de matériaux de génie civil à faibles impacts environnementaux. INSA de Rennes, 2004.

[Collet 2013] Collet, F., Chamoin, J., Pretot, S., Lanos, C.; Comparison of the hygric behaviour of three hemp concretes. Energy and Buildings, 2013, 62, 294–303.

[Collet 2014a] Collet, F., Pretot, S; Thermal conductivity of hemp concretes: Variation with formulation, density and water content. Construction and Building Materials, 2014, 65, 612–619.

[Collet 2014b] Collet, F., Pretot, S; Experimental highlight of hygrothermal phenomena in hemp concrete wall. Building and Environment, 2014, 82, 459–466.

[Damfeu 2016] Damfeu, J.C., Meukam, P., Jannot, Y; Modeling and measuring of the thermal properties of insulating vegetable fibers by the asymmetrical hot plate method and the radial flux method: Kapok, coconut, groundnut shell fiber and rattan. Thermochimica Acta, 2016, 630, 64–77.

[De Bruijn 2013] De Bruijn, P., Johansson, P.; Moisture fixation and thermal properties of lime–hemp concrete. Construction and Building Materials, 2013, 47, 1235–1242.

[Dinh 2015] Dinh, T.M., Magniont, C., Coutand, M., Escadeillas, G; Hemp concrete using innovative pozzolanic binder, First International Conference on Bio-based Building Materials, June 22-24 2015, Clermont-Ferrand, France, 265-270.

[Dupont 2014] Dupont, C., Chiriac, R., Gauthier, G., Toche, F; Heat capacity measurements of various biomass types and pyrolysis residues. Fuel, 2014, 115, 644–651.

[Evrard 2008] Evrard, A., 2008: Transient hygrothermal behaviour of Lime-Hemp Materials. Université Catholique de Louvain, 2008.

[Evrard 2010] Evrard, A., De Herde, A; Hygrothermal Performance of Lime-Hemp Wall Assemblies. Journal of Building Physics, 2010, 34, 5–25.

[Groupe RBR 2020-2050] Groupe RBR 2020-2050; Cap sur le futur « Bâtiment responsable » - Rapport de recommandations #3. Plan Bâtiment Durable, 2014.

[Gourlay 2016] Gourlay, E., Glé, P., Marceau, S., Foy, C., Moscardelli, S.; Effect of water content on the acoustical and thermal properties of hemp concretes. Construction and Building Materials, 2016.

[Le 2015] Le, A.D.T., Samri, D., Rahim, M., Douzane, O. et al.; Effect of Temperature-dependent Sorption Characteristics on The Hygrothermal Behavior of Hemp Concrete. 6th International Building Physics Conference, IBPC, Torino, Italy, June 14-17 2015, Energy Procedia, 78, 1449–1454.

[Maalouf 2014] Maalouf, C., Le, A.D.T., Umurigirwa, S.B., Lachi, M. et al.; Study of hygrothermal behaviour of a hemp concrete building envelope under summer conditions in France. Energy and Buildings, 2014, 77, 48–57.

[Magniont 2012] Magniont, C., Escadeillas, G., Coutand, M., Oms-Multon, C; Use of plant aggregates in building ecomaterials. European Journal of Environmental and Civil Engineering, 2012, 16, 17–s33.

[Nguyen 2010] Nguyen, T.T.; Contribution à l'étude de la formulation et du procédé de fabrication d'éléments de construction en béton de chanvre. Université de Bretagne-Sud, 2010.

[Nozahic 2012] Nozahic, V.; Vers une nouvelle démarche de conception des bétons de végétaux lignocellulosiques basée sur la compréhension et l'amélioration de l'interface liant/végétal - Application à des granulats de chènevotte et de tige de tournesol associés à un liant ponce/chaux. Université Blaise Pascal - Clermont II, 2012.

[Osanyintola 2006] Osanyintola, O.F., Simonson, C.J; Moisture buffering capacity of hygroscopic building materials: Experimental facilities and energy impact. Energy and Buildings, 2006, 38, 1270–1282.

[Pierre 2013] Pierre, T., Colinart, T., Glouannec, P. Measurement of Thermal Properties of Biosourced Building Materials. Int J Thermophys, 2013, 35, 1832–1852.

[Rahim 2016a] Rahim, M., Douzane, O., Tran Le, A.D., Langlet, T. Effect of moisture and temperature on thermal properties of three bio-based materials. Construction and Building Materials, 2016, 111, 119–127.

[Rahim 2016b] Rahim, M., Douzane, O., Tran Le, A.D., Promis, G. et al.; Characterization and comparison of hygric properties of rape straw concrete and hemp concrete. Construction and Building Materials, 2016, 102, Part 1, 679–687.

[SOeS 2016] Service de l'observation et des statistiques (SOeS); Chiffres clés de l'énergie (No. Edition 2015). Commissariat général au développement durable, 2016.

[Surface Measurement Systems 2000] Surface Measurement Systems; DVS Manual, 2000.

[Vololonirina 2016] Vololonirina, O., Perrin, B; Inquiries into the measurement of vapour permeability of permeable materials. Construction and Building Materials, 2016, 102, Part 1, 338–348.

[Walker 2014] Walker, R., Pavía, S; Moisture transfer and thermal properties of hemp–lime concretes. Construction and Building Materials, 2014, 64, 270–276.

[Woloszyn 2009] Woloszyn, M., Kalamees, T., Olivier Abadie, M., Steeman, M. et al.; The effect of combining a relative-humidity-sensitive ventilation system with the moisture-buffering capacity of materials on indoor climate and energy efficiency of buildings. Building and Environment, 2009, 44, 515–524.